Available online at www.sciencedirect.com
SCIENCE DIRECT®
Biochemical and Biophysical Research Communications 306 (2003) 198–207
BBRC
www.elsevier.com/locate/ybbrc

Cloning, sequencing, and characterization of the murine *nm23*-M5 gene during mouse spermatogenesis and spermiogenesis☆

Kyu-Chan Hwang,[a,b] Do-Won Ok,[a,b] Jong-Chan Hong,[b] Myeong-Ok Kim,[b] and Jin-Hoi Kim[a,b,*]

[a] *Major of Dairy Science, College of Agriculture, Gyeongsang National University, Chinju, GyeongNam 660-701, Republic of Korea*
[b] *Division of Applied Life Science, Gyeongsang National University, Chinju, GyeongNam 660-701, Republic of Korea*

Received 21 April 2003

Abstract

Nucleoside diphosphate kinases (NDPKs) are conserved throughout evolution and have been shown to be involved in various biological phenomena. By functional screening in yeast, we identified a new member of the NDPK family, *nm23*-M5, which encodes a 211-amino acid protein with 86% identity to the human homolog *Nm23*-H5. Northern blot analysis revealed that *nm23*-M5 encodes two transcripts of 0.8 and 0.7 kb, which are highly and specifically expressed in adult testis. Reverse transcriptase polymerase chain reaction (RT-PCR) analysis showed that *nm23*-M5 transcripts first appear in pachytene spermatocytes and increase in abundance in subsequent stages. However, a low level of *nm23*-M5 mRNA was detected by RT-PCR in other tissues, such as ovary, brain, heart, and kidney. In situ hybridization studies showed that testicular *nm23*-M5 transcripts are localized in stage 12 to stage 16 spermatids in the neighboring lumen of seminiferous tubules. This distribution contrasts with that of *Nm23*-H5 transcripts, which are specifically found in spermatogonia and early spermatocytes. The heterologous expression of *nm23*-M5 in yeast cells confers protection from cell death induced by *Bax*, which is due to the generation of reactive oxygen species. Furthermore, overexpression of *nm23*-M5 in fibroblasts altered the cellular levels of several antioxidant enzymes, particularly glutathione peroxidase 5. Thus, we believe that the murine *nm23*-M5 gene plays an important role in late spermiogenesis by elevating the ability of late-stage spermatids to eliminate reactive oxygen species.

Keywords: *nm23*-M5; NDP kinase; Spermatogenesis; Stage-specific; Testis; GPX; Antioxidants

Nucleoside diphosphate kinases (NDPKs) (EC 2.7.4.6) are found in animals and plants throughout evolution and catalyze the transfer of γ-phosphates between nucleoside and deoxynucleoside di- and triphosphates. Apart from their role in nucleotide synthesis, the NDPKs in mammalian cells are also involved in various processes, such as tumor metastasis, cell proliferation, transcriptional regulation, development, senescence, and apoptosis [1–5].

A number of mammalian genes that encode NDPK-like molecules (denoted *non-metastatic 23* or *nm23* genes) have been identified. The first *nm23* gene was isolated on the basis of its reduced level of expression in highly metastatic murine melanomas and was therefore proposed to be a metastatic suppressor gene [6]. Since then, several murine *nm23* genes (*nm23*-M1 to *nm23*-M7) and human *Nm23* genes (*Nm23*-H1 to *Nm23*-H8) have been cloned [5,7–11]. Of the human genes, the *Nm23*-H1 gene product was characterized as the human NDPK α isoform, while *Nm23*-H2 was identified as the NDPK β isoform [12]. NM23-H5 appears to differ from the other human NDPKs in several aspects. First, it lacks two important catalytic site residues and thus does not appear to possess NDPK activity [8]. Second, the *Nm23*-H5 gene is transcribed primarily in the testis, especially in spermatogonia and early spermatocytes [8].

☆ *Abbreviations:* CAT, catalase; EST, expressed sequence tag; GAPDH, glyceraldehyde-3-phosphate dehydrogenase; GPX, glutathione peroxidase; kb, kilobase; NDPK, nucleoside diphosphate kinase; Nm23, non-metastatic 23; PCR, polymerase chain reaction; RT-PCR, reverse transcription PCR; SOD, superoxide dismutase.

* Corresponding author. Fax: +82-55-751-5410.
E-mail address: jinhoi@nongae.gsnu.ac.kr (J.-H. Kim).

0006-291X/03/$ - see front matter © 2003 Elsevier Science (USA). All rights reserved.
doi:10.1016/S0006-291X(03)00916-1

This contrasts with the expression patterns of many NDPKs, which are usually expressed abundantly in most tissues. Therefore, the function of NM23-H5 is still unknown.

The testis is sensitive to a variety of stressors, such as hyperthermia, inflammation, radiation, and exposure to agents that induce the apoptosis of germ cells [13–16]. Since oxidative stress in the testis is one of the major factors that induce germ cell apoptosis, this organ has fairly high concentrations of antioxidants such as GPX, ascorbic acid, and vitamin E [17,18]. These antioxidants protect germ cells against oxidative DNA damage [19] and thus may play important roles in spermatogenesis. Supporting this notion is that deficiencies in ascorbic acid and vitamin E result in disturbances in spermatogenesis [20,21]. Thus, the testis has a mechanism that it uses to defend itself from oxidative stress. This mechanism thus plays critical roles in the maintenance of spermatogenesis and spermiogenesis.

We wished to characterize the factors that help the testis to resist oxidative stress stimuli, in particular, apoptosis-inducing reactive oxygen species (ROS). We thus screened a mouse testis library for clones whose expression in yeast inhibited cell death promoted by the co-expression of *Bax*. *Bax* induces apoptosis due to the generation of ROS [22]. We found that *nm23*-M5 conferred the highest tolerance to *Bax*-induced cell death. We characterized the gene expression patterns of *nm23*-M5 and found that it is specifically expressed in late-stage spermatids. We speculate that *nm23*-M5 expression may promote the survival of developing male germ cells by upregulating their antioxidant mechanisms. Supporting this notion is that expression of *nm23*-M5 in NIH3T3 cells elevated the transcript levels of several antioxidant enzymes in these cells.

Materials and methods

Enzymes, vectors, and reagents. [α-^{32}P]dCTP (>3000 Ci/mmol) was purchased from NEN (Boston, MA, USA). DNA modifying enzymes, restriction enzymes, the DNA polymerase I large fragment (Klenow fragment), and a random labeling kit were from Boehringer–Mannheim (Heidelberg, Germany). Nitrocellulose membranes were from Millipore (Marlborough, MA, USA) and filter papers were from Whatman (Hillsboro, OR, USA). Chloroform and methanol were from Merck (Germany). Premix *Taq* polymerase and LA polymerase were from Takara (Shiga, Japan), DNA size markers were from AT-Gene (Daejon, Korea), and the pBluescript SK$^-$ vector was from Promega. The plasmid isolation kits were from Qiagen (Valencia, CA, USA). All molecular biological procedures, including agarose gel electrophoresis, restriction enzyme digestion, ligation, bacterial transformation, and preparation of competent cells, were performed according to standard methods [23].

Screening strategy. Screening strategy is performed according to previous reported method [23]. In brief, the pADGal4-2.1 vector (Stratagene) containing the mouse testis cDNA library was transformed into the W303-1a strain harboring pGilda-Bax. The transformed cells (5×10^6) were plated onto galactose-based synthetic minimal medium (SD) [0.67% yeast nitrogen base, 2% galactose, and (10×) amino acids dropout solution] that is deficient in leucine and histidine. The growing colonies were selected and subcloned in pGEM-T easy vector.

Cloning of nm23-M5 cDNA. For cloning of long *nm23*-M5 mRNA, a search in the GenBank sequence data base for expressed sequence tags (EST) that are homologous to the NME5 sequence (AF343565) identified several EST-encoded proteins that are homologous to but different from the sequences of the *nm23* gene products identified so far. Specific primers whose sequences were deduced from EST AK006111 (5′-AAC ACC TGA ACA GAG CTG ATT-3′) and EST AV204912 (anti 5′-ACA TAT ATG CTT TTA ATG TAA AGA-3′) were used for PCR amplification. The three amplification products (811, 710, and 504 bp) were subcloned in the pGEM-T easy vector using the TA cloning kit from Promega and sequenced automatically (Applied Biosystems, ABI).

Northern blot analysis. Total RNA was isolated from various tissues using TRIZOL reagent (Gibco-BRL). Northern blot analysis was performed as previously described using random-labeled *nm23-M5* cDNA. Briefly, 20 μg of total RNA was denatured in 68% formamide and 2.2 M formaldehyde for 15 min at 65 °C and subjected to electrophoresis in a 1.2% agarose/formaldehyde gel. The total RNA was then transferred to a membrane and prehybridized with hybridization buffer for 3 h. The probe was labeled with [α-^{32}P]dCTP. After adding the labeled probe, hybridization was carried out for 24 h at 68 °C with the same buffer as that used for prehybridization. The membranes were washed for 10 min at 37 °C with 2× SSC/0.1% SDS (2× SSC = 0.3 M NaCl/0.03 M sodium citrate, pH 7.0) and then for 10 min at 65 °C with 0.2× SSC/0.1% SDS. Autoradiograms were quantified with an imaging densitometer by Molecular Analyst software (Bio-Rad Laboratory, model GS-700).

Determination of intron boundaries and sizes. Oligonucleotide primers used for sequencing were designed according to the *nm23*-M5 cDNA sequence to determine the genomic structure of *nm23*-M5: 5′-GGA TCT GGA TTC ACC ATT ATT C-3′ and anti 5′-CAG GTG TAG TTT CCG TCT-3′ for intron 2, 5′-AAG GAG ACA CAC CCG GAC AG-3′ and anti 5′-GTA CCG TAT ATC GCC CTT AAG-3′ for intron 3, 5′-GAT CAG GTT CAT GTT TCC AGC-3′ and anti 5′-CCA ATT GGA ATG GGT TCA ATA ATC-3′ for intron 4, and 5′-AAG GAA AAG CCA CCA GAC CCT-3′ and anti 5′-CAG CCA ATC AGC GAG CCA-3′ for intron 5. Genome structure was identified by PCR followed by 0.8% agarose gel electrophoresis. All sequencing analyses were performed using an ABI automated sequencer (ABI377 DNA sequencer, Applied Biosystems) according to the manufacturer's protocols.

Animals and tissue preparations. Male mice ($n = 10$, 40 g/body weight, Gyeongsang National University Animal Breeding Center, Chinju, Korea) were housed in a temperature-controlled environment under a 14 h lighting regime with food ad libitum. For in situ hybridization, the testes were aseptically dissected, fixed in ice-cold 4% neutral buffered paraformaldehyde (NBP) for 48 h, and cryoprotected by immersion into 20% sucrose phosphate buffer for 24 h at 4 °C. Tissues were frozen in O.C.T. compound (A.O. Co) and 10 μm coronal sections were prepared (Leica cryostat CM 3050C, Germany). Sections were thaw-mounted on probe-on plus charged slides (Fisher) at room temperature and stored at −70 °C until use.

Synthesis of cRNA probes. The full-length mouse *nm23*-M5 cDNA clone was isolated by functional screening in yeast. An 811 bp fragment encoding the full-length cDNA of *nm23*-M5 was cloned into the RNA-synthesizing vector pGEM-T Easy vector (Promega), which contains a polylinker and the promoters for the T7 and SP6 polymerases. The cDNA was then analyzed by sequencing (Sequenase 2.0; USB). In situ probes were synthesized from pGEM-T Easy vector recombinant subclones. Antisense *nm23*-M5 cRNA probes were transcribed with SP6 RNA polymerase from the pGEM-*nm23*-M5 construct linearized with *Nco*I and sense *nm23*-M5 cRNA probes were transcribed with T7 RNA polymerase. [^{35}S]UTP-labeled probes with a specific activity of

1.0×10^9 cpm/μg were prepared using an in vitro transcription kit (Promega). Antisense and sense cRNA probes were purified on Sephadex G-50 DNA grade columns and eluted with SET buffer (0.1% SDS, 1 mM EDTA, 10 mM Tris, and 10 mM DTT). Polyacrylamide gel analysis of purified probes revealed that >90% of the probes were of the expected length.

Busulfan treatment. Twenty ICR male mice and ten W/W^v mutant mice (SLC, Japan) ranging in age from 7 to 14 weeks were used. Eight weeks old ICR male mice received a single intraperitoneal injection with busulfan (40 mg/kg body weight) diluted in sesame oil as previously described [26]. The levels of *nm23*-M5 expression were measured 1–7 weeks after busulfan treatment in all experiments. Mice (30–40 g, 7–14 weeks old) were housed in wire cages and fed ad libitum. The mice were maintained at 22 ± 1 °C under 12 h light and dark cycles with 70% humidity. Animals were maintained and experiments were conducted in accordance with the Gyeongsang National University guide for the Care and Use of Laboratory Animals.

In situ hybridization. After the slides were removed from the −80 °C deep freezer, they were air-dried at room temperature and washed in 2× sodium chloride–sodium citrate (SSC; 0.5 M NaCl; 0.3 M sodium citrate, pH 7.0) buffer. Proteinase K treatment and acetylation of the tissues were performed essentially as described by Angerer et al. [24] and Kim et al. [25]. The sections were covered with prehybridization buffer and incubated at 37 °C for 1 h. After the prehybridization buffer was removed, the slides were covered with hybridization buffer (prehybridization buffer plus probes). Hybridization with antisense or sense probes was performed by adding 50 μg/ml yeast tRNA, 10 mM dithiothreitol, and 6×10^5 cpm of RNA probe per microliter of solution. Coverslips were placed over the slides and the slides were incubated at 60 °C for 24 h. The slides were then incubated in a posthybridization buffer, dipped in NTB2 emulsion (1:1 dilution, Kodak), exposed for two weeks at 4 °C, developed in D19 developer (1:1 dilution, Kodak) at 15 °C, and counterstained with cresyl violet. Slides were observed by dark- and bright-field microscopy.

Cell culture and transfection. The *nm23*-M5 cDNA was inserted into the *Not*I-digested pRc/CMV expression vector (pRc/CMV-*nm23*-M5). The resulting plasmid was used to transfect NIH3T3 cells maintained in Dulbecco's modified Eagle's medium containing 10% fetal calf serum. Thus, after the NIH3T3 cells had been allowed to grow to 50% confluence, they were transfected with 1 μg of the linear pRc/CMV-*nm23*-M5 expression vector by using Effectene (Qiagen, Valencia, CA, USA) according to the manufacturer's protocols. Control cells were simultaneously transfected with the pRc/CMV-*neo* vector lacking *nm23*-M5 cDNA insert. After transfection, the cells were selected in a medium containing 0.7 μg/ml geneticin (G418).

Reverse transcriptase-polymerase chain reaction. For the first strand cDNA synthesis, a reverse transcription reaction was performed on 2 μg of the total RNA prepared from each cell pellet in a final volume of 20 μl. The RT mix contained 1× RT buffer, 10 mM dithiothreitol (DTT), 0.5 mM of each dNTP, 0.5 μg oligo(dT), 10 units RNasin ribonuclease inhibitor, and 200 units superscript reverse transcriptase. The reverse transcription reaction was carried out at 42 °C for 50 min followed by heating at 70 °C for 15 min to inactivate the reaction. The mixtures were then stored at 4 °C until use in PCR. Reverse transcriptase-polymerase chain reaction (RT-PCR) experiments were repeated at least three times to assess the reproducibility of the results. PCR analysis was performed in a final volume of 50 μl containing the cDNA sample, 2 mM $MgCl_2$, 50 mM KCl, 10 mM Tris–HCl (pH 8.3), 1.2 mM of each dNTP, 0.4 μM of each primer, and 2 units *Taq* polymerase (ATgene). The amplification of *nm23*-M5 partial cDNA (636 bp) was performed with specific primers (5′-ATG GTG GTA TCA ATG CCC CTG-3′and anti 5′-CTA AGG CTC TTC TGT CAC TGG G-3′). The sequences of the primers for antioxidant enzymes, RAD51, and GAPDH are summarized in Table 1. For each RT-PCR

Table 1
Primer sequences used in RT-PCR analysis of the expression of antioxidant enzymes, RAD51, and *GAPDH*

Gene		Primer sequence	Products size (bp)	GenBank Accession Nos.
SOD1	Sense	5′-ATGGCGATGAAAGCGGTGTG-3′	518	X06683
	Antisense	5′-TAATGGTTTGAGGGTAGCAGAT-3′		
SOD2	Sense	5′-CTCCCAGACCTGCCTTACG-3′	488	BC010548
	Antisense	5′-TAGTAAGCGTGCTCCCACAC-3′		
SOD3	Sense	5′-GACGAAGGGAGGTGGATGCT-3′	753	U38261
	Antisense	5′-AGGTTCGTGGAGGCATCTG-3′		
CAT	Sense	5′-CTGTGAACTGTCCCTACCGC-3′	583	BC013447
	Antisense	5′-TCCAGCGTTGATTACAGGTGAT-3′		
GPX1	Sense	5′-CGTTTGAGTCCCAACATCTC-3′	512	NM_008160
	Antisense	5′-TCAAAGTTCCAGGCAATGTCG-3′		
GPX2	Sense	5′-GAGCATCCTGTCTTTGCCTAC-3′	476	NM_030677
	Antisense	5′-AGGGTTTAGGAAGATGCCATCAT-3′		
GPX3	Sense	5′-TGGGAACCCATGAAGATCCAT- 3′	513	NM_008161
	Antisense	5′-TGAGCAGAACCATTGGACCTA-3′		
GPX4	Sense	5′-AGGGCGGGCAAGCCATACT-3′	539	D87896
	Antisense	5′-CCCTTGGGCTGGACTTTCAT-3′		
GPX5	Sense	5′-GAGGTTTGGCTGAGTATGTTA-3′	532	NM_010343
	Antisense	5′-ACAGAAAGGAGCACTTATGCAG-3′		
RAD51	Sense	5′-GTTACCATACAGTGGAGGCTGT- 3′	665	NM_011234
	Antisense	5′-GGTGATTACCACTGCGACAC-3′		
GAPDH	Sense	5′-GTGAAGGTCGGTGTGAACGG- 3′	620	NM_008084
	Antisense	5′-GATGCAGGGATGATGTTCTG-3′		

analysis, internal glyceraldehyde-3-phosphate dehydrogenase (GAPDH) and negative (blank) controls were included. After a first denaturation step of 3 min at 94 °C, 30–38 amplification cycles were performed. Each cycle involved denaturation at 94 °C for 30 s, annealing at 55 °C for 30 s, and extension at 72 °C for 1 min. A final extension step of 10 min at 72 °C was performed to complete the PCR.

Results

Identification of the murine nm23-M5 gene

In this study, we cloned a new murine NDPK, *nm23*-M5. This gene was identified when, in an effort to characterize *Bax*-induced apoptosis in animal cells, we screened a mouse testis library for clones whose expression inhibited the *Bax*-promoted cell death of yeast. Thus, the yeast strain W303-1a was co-transformed with a murine testis cDNA library and *Bax*, and 5×10^6 transformants were screened. The *Bax*-resistant transformants were selected on medium containing galactose and restriction analysis defined 39 clones that were denoted testis-1 to testis-39. Since testis-12 conferred the highest tolerance to *Bax*-induced cell death (Fig. 1), this clone was selected for further study. It was sequenced and this cDNA sequence has been deposited in GenBank (Accession No. AF343565) (Fig. 2A). This protein was designated Nm23-M5 based on (i) the alignment of the derived protein sequence with the protein sequences of other members of the family, including those of other species and (ii) the evaluation of the phylogenetic tree (Figs. 2B and C). Nm23-M5 shares 86% identify with its human counterpart NM23-H5. However, it shares only 18.3–20.1% identity with the other five murine kinases.

The *nm23*-M5 cDNA contains a 5′ untranslated region of 95 bp, an open reading frame of 633 bp that was predicted to encode a protein of 211 amino acid residues, and a 3′ untranslated region of 56 bp (Fig. 2A). The deduced protein has a molecular mass of 23,971 Da and a calculated p*I* of 5.88, indicating that it is an acidic protein. Nm23-M5 is unique in the NDPK family in that it possesses a COOH extension.

Testis-specific expression of the nm23-M5 gene

To determine the tissue distribution of *nm23*-M5 expression, we performed RT-PCR assays. The gene is expressed predominantly in the testis, but low levels of transcript can be detected in the ovary, heart, kidney, and brain. Oligonucleotide primers specific for *nm* 23-M5 transcripts amplified two isoforms (811 and 504 nt) from the cDNA of the ovary, heart, kidney, and brain, but three isoforms (811, 710, and 504 nt) from the testicular cDNA (Fig. 3B). The longest 811bp form encodes 211 amino acids and is designated as 'full.' The shorter 710 and 504 nt forms encode 114 and 43 amino acids, respectively, due to an in-frame stop codon. They were designated as delE4 and delE3E4, respectively (Fig. 3C). Sequence analysis of *nm23*-M5 gene revealed that these isoforms lack the exon 3 alone or both of exons 3 and 4, respectively. Northern hybridization also revealed that two *nm*23-M5 transcripts of 0.8 and 0.7 kb are predominantly expressed in the testis. The difference of RT-PCR and Northern blot analysis may be caused by low expression of delE3E4 isoform. Taken together, our results suggested that the *nm23*-M5 isoforms were resulted from alternative splicing (Figs. 3B and C).

Localization of nm23-M5 expression in the testis

The cellular localization of the *nm23*-M5 transcript was determined by in situ hybridization of ^{35}S-labeled cRNA antisense probes to histological sections. Under low-magnification dark-field illumination, a strong hybridization signal (white grains) was detected with the antisense probe (Fig. 4B), but not with the sense probe (Fig. 4A). The intensity of the *nm23*-M5 hybridization signal varied substantially among different seminiferous

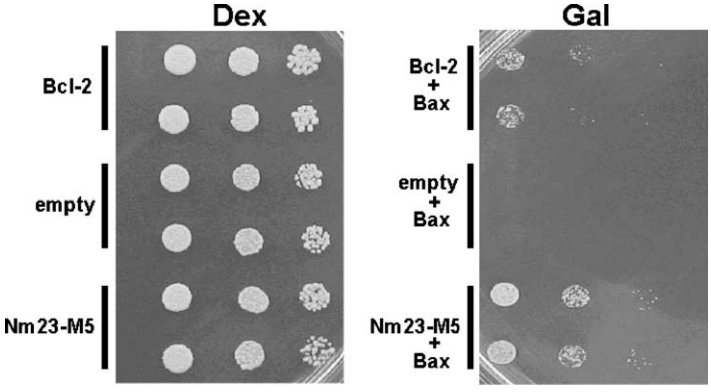

Fig. 1. The *nm23*-M5 gene suppresses *Bax*-induced cell death in yeast. W303-1a cells harboring either pGilda-*Bax*/pADGal4-2.1-*Bcl-2* (upper), pGilda-*Bax*/pADGal4-2.1 (middle), or pGilda-*Bax*/pADGal4-2.1-*nm23*-M5 (lower) were placed onto SD-glucose (Dex) or SD-galactose (Gal)-containing plates by spotting aliquots (5 μl) of 10-folds serially diluted cultures that had been grown until an OD_{600} of 0.3. Plates were photographed after a 2 day incubation at 30 °C.

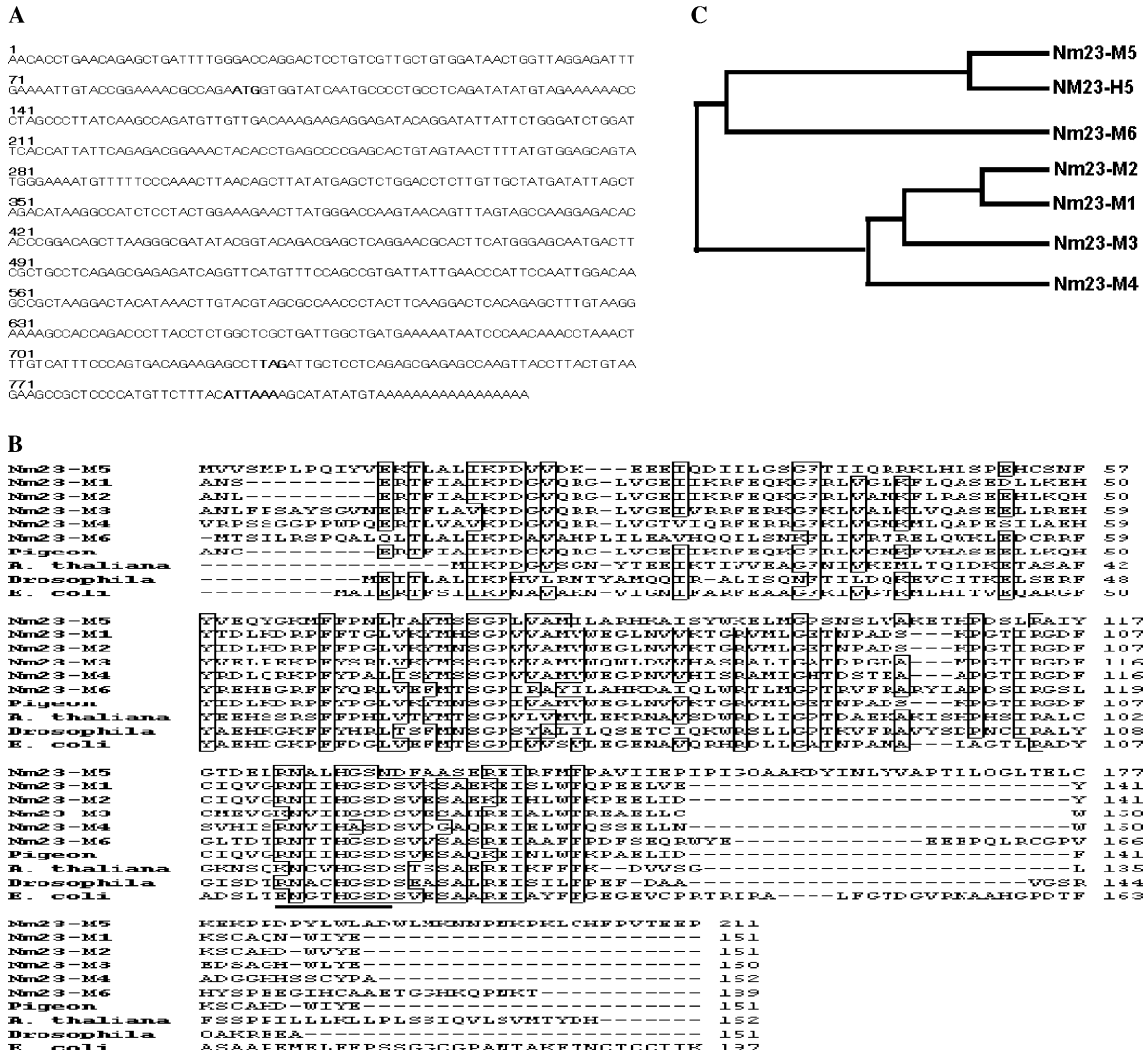

Fig. 2. The *nm23*-M5 cDNA and protein sequences. (A) Nucleotide sequence. The sequence has been deposited in GenBank (Accession No. AF343565). The start site, stop site, and polyadenylation signal are shown in bold. Nucleotides are numbered on the left. (B) Comparison of the Nm23-M5 amino acid sequence with that of NDPKs from different organisms. Black backgrounds indicate an identical amino acid shared by at least five proteins. Gaps are indicated by a hyphen. The NDPK consensus motif (NXXHG/ASD) is underlined. Accession Nos. are as follows: Nm23-M1 (P15532), Nm23-M2 (S29241), Nm23-M3 (Q9WV85), Nm23-M4 (Q9WV84), Nm23-M5 (AAK20866), pigeon (Q90380), *Arabidopsis thaliana* (NM-101602), *Drosophila melanogaster* (XP_082653), and *Escherichia coli* (NP_289071). The alignment was prepared using BioEdit version 5.0.9. (C) Phylogenetic analysis of NDPK proteins drawn with the CLUSTALX program.

tubules, indicating that the expression of *nm23*-M5 is stage-specific. High-magnification of bright- and dark-field illumination revealed that high-level *nm23*-M5 expression is confined to late spermatids, depending on the stage of tubules, and is not observed outside of the testicular tubules (Figs. 4C, E, and F). An accumulation of grains was detected in the neck region of late-stage spermatids. By observing neighboring sections stained with hematoxylin-eosin, the specific seminiferous tubules were identified as being stage XII tubules because they contained zygotene and metaphase spermatocytes. Scattered autoradiographic grains were detected mainly in stage 12-stage 16 spermatids, and the strongest signals were detected concomitantly with the appearance of late spermatids in the neighboring lumen.

We also investigated the cellular and temporal profiles of *nm23*-M5 expression during the course of pubertal testicular development. *Nm23*-M5 expression was first detected at day 15 after birth, a time when primary spermatocytes in the early pachytene stage of meiosis are the most advanced germ cells present in the testis (Fig. 5A). To confirm that *nm23*-M5 mRNA is indeed expressed in pachytene spermatocytes, male mice (7 weeks age old) were treated with busulfan, which destroys developing male germ cells. This is followed by regenerated spermatogenesis and spermiogenesis after arrest of a transit period (Fig. 5C) [26]. Testicular weight increased steadily in control animals from the beginning (7 weeks old) to the end of the experiment (14 weeks age old). In contrast, the testicular weight of busulfan-trea-

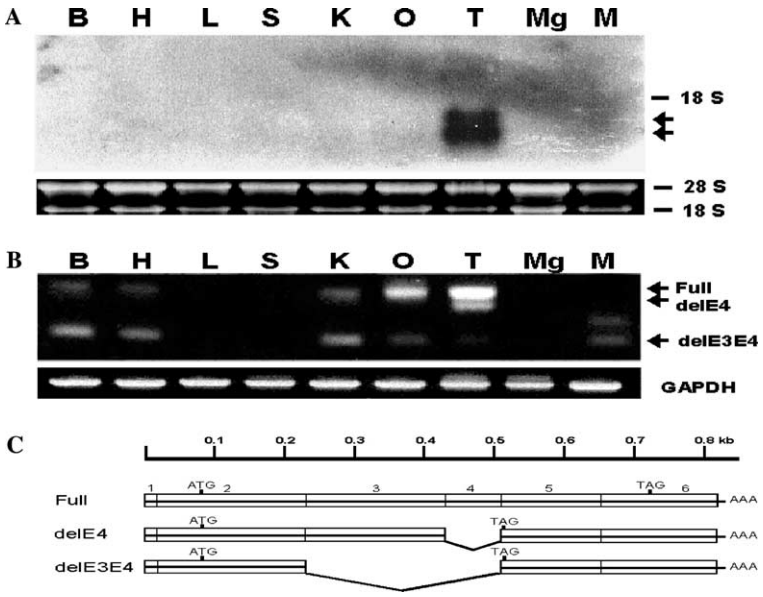

Fig. 3. Analysis of *nm23*-M5 mRNA in various murine tissues. (A) Northern blot analysis of total RNA from murine tissues probed with random-labeled *nm23*-M5. The arrow indicates the mouse *nm23*-M5 signal. The ethidium bromide-stained gel confirms that approximately equal amounts of total RNA are loaded in each lane. (B) RT-PCR analysis of the distribution of nm23-M5 mRNA in murine tissues. (C) Schematic representation of the full-length mouse *nm23*-M5 and the two alternatively spliced forms identified in the testis. The exons are represented by white squares. B, brain; H, heart; Mg, mammary gland; S, spleen; L, liver; O, ovary; T, testis; M, muscle; and K, kidney.

ted mice dropped a week after treatment and was low at four weeks after busulfan injection (33% of control value). Pachytene spermatocytes in testis sections could be re-detected at 7 weeks after busulfan treatment, but not at 4 weeks (Fig. 5D). This was matched by the RT-PCR data, which showed that at 4 weeks after treatment, neither *nm23*-M5 nor *RAD51*, which is expressed exclusively in pachytene spermatocytes [27,28], was expressed in the busulfan-treated testes (Fig. 5B): both genes began to be re-expressed again 7 weeks after treatment when pachytene spermatocytes are re-generated in testis (Figs. 5C and D). Furthermore, the highest level of expression was observed in adult mice, but not in *c-kit* mutant mice (W/W^v), which have only spermatogonia and somatic cells. This result indicates that *nm23*-M5 is highly and specifically expressed in male germ cells, specifically those ranging in development from pachytene spermatocytes to haploid germ cells, but not in testicular somatic cells.

Determination of the genomic structure of nm23-M5

The genomic structure of *nm23*-M5 gene is shown in Fig. 6. The template DNA used for PCR amplification was isolated from a BAC genomic library. The positions of the exon/intron boundaries were determined by sequence of PCR products amplified with oligonucleotide primers that are specific to the coding sequences of the gene, respectively (Fig. 6B). When intron sizes were estimated by PCR, the *nm23*-M5 gene spans at least 17 kb and consists of 6 exons and 5 introns (Fig. 6). All the intron boundaries follow the gt-ag rule. The sequences that flank the exon/intron boundaries in the *nm23*-M5 gene are shown in Fig. 6B. In addition, the ATG translation start site is at position 82 in exon 2. Genomic Southern analysis showed that *nm23*-M5 is a single copy gene.

Overexpression of antioxidant enzymes in NIH-3T3 cells that overexpress nm23-M5

We hypothesized that *nm23*-M5 might serve to protect the testis from oxidative stress. To test this, we examined whether overexpression of this gene in NIH3T3 fibroblasts, which do not express the *nm23*-M5 gene, would enhance antioxidant activity in order to suppress ROS-induced apoptosis. The *nm23*-M5-expressing NIH3T3 line was established by transfection with an expression vector that contains mouse *nm23*-M5 cDNA under control of the cytomegalovirus promoter (CMV/*nm23*-M5). A control NIH3T3 line was transfected with the CMV-neo expression vector alone. We assessed the transcript levels of nine antioxidant enzymes, including those belonging to the superoxide dismutase (SOD), catalase, and glutathione peroxidase (GPX) families (Table 1). As shown in Fig. 7A, the CMV-neo- and CMV/*nm23*-M5-transfected cells showed different expression profiles of antioxidant enzymes. First, SOD2 and GPX2 expression in CMV/*nm23*-M5 transfected cells was increased by 33% and 28%, respectively, compared to the CMV-neo control. Furthermore, GPX5, which converts hydrogen peroxide into water,

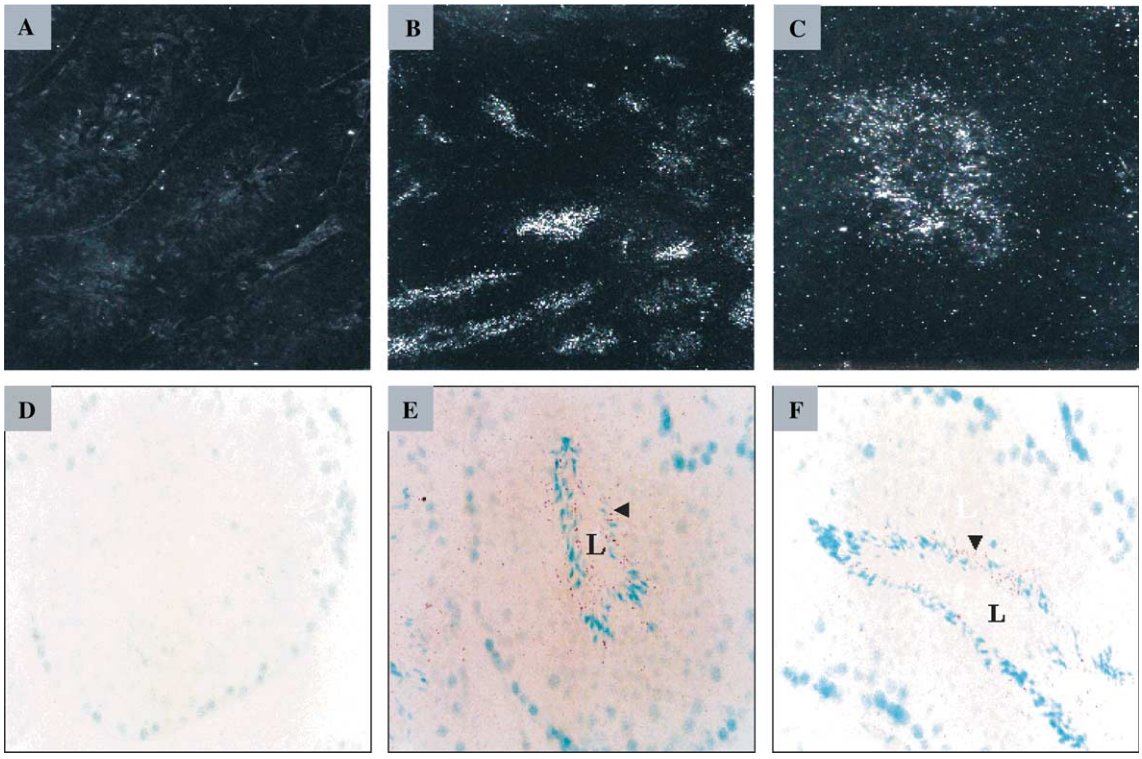

Fig. 4. In situ hybridization analysis of *nm23*-M5 expression in testicular histological sections. For details, see Materials and methods. Shown are dark-field digital micrographs of sectioned adult testes that were hybridized with sense (A) or antisense (B) *nm23*-M5 RNA probes. Note that the different seminiferous tubules in (B) show varying densities of the white grains on the autoradiogram, whereas these grains are barely visible in the section shown in (A). (C–F) Higher magnification of the areas indicated in (B). (C) indicates high-magnification bright and dark-field micrographs of the same section as shown in (B). Accumulations of silver grains indicative of *nm23*-M5 mRNA appear as dark dots mainly in stages V–VI (E and F) and are not visible in other tubules at this magnification (D). Magnification: 50× (A and B); 200× (C–F).

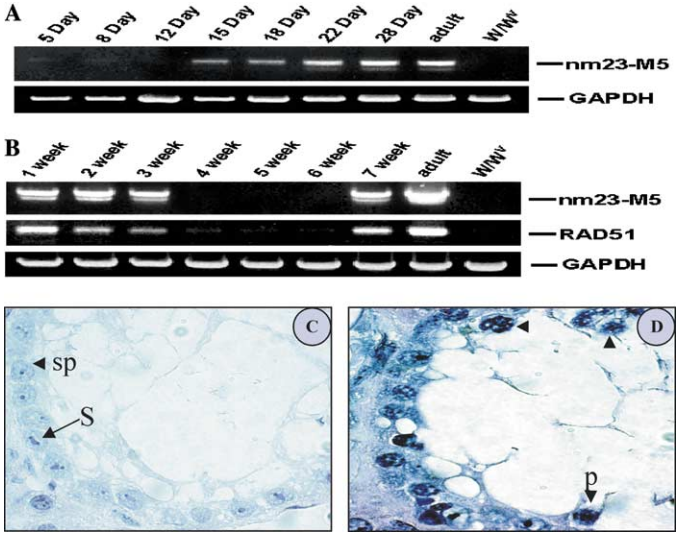

Fig. 5. Temporal pattern of expression of *nm23*-M5. (A) RT-PCR was performed with testis-derived RNAs expressed at different developmental stages. Total RNAs were isolated from the mouse testis at the indicated days postpartum (5, 8, 12, 15, 18, 22, and 28 days, adult, and W/W^v). Stages were classified according to [34]. (B) Comparison of the patterns of expression of *nm23*-M5 and *RAD51* (pachytene-specific biomarker) by RT-PCR using RNAs derived from the testes of busulfan-treated adult mice (from 7 to 14 weeks old) taken 1, 2, 3, 4, 5, 6, and 7 weeks after treatment. A 7 weeks old adult testis and a testis from a 7 weeks old W/W^v mouse were also tested. (C) and (D) show the histological appearance of the testes at 4 or 7 weeks after busulfan treatment, respectively. Sp, spermatogonia, S, Sertoli cell, and p, pachytene spermatocyte (arrow). Murine GAPDH was used as a control to confirm the integrity of the mRNA samples.

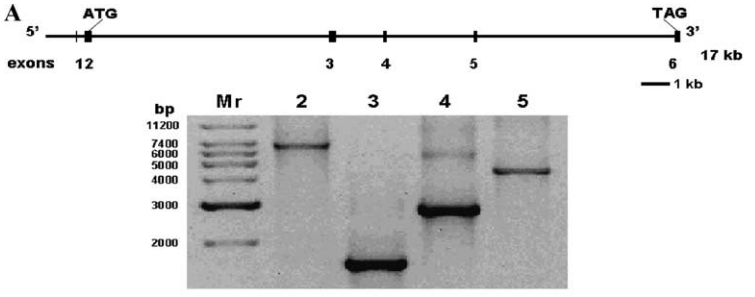

B

Exon	Size	3' Splice site intron/exon	5' Splice site exon/intron	Intron size
1	>14 bp	5' UTR	CCTGAACAGA/gtaagtaaag	309 bp
2	210 bp	tttgccacag/GCTGATTTTG	CATTATTCAG/gtaacgtctg	6896 bp
3	206 bp	ttgtttacag/AGACGGAAAC	ACCCGGACAG/gtaatttcca	1557 bp
4	101 bp	ttctctctag/CTTAAGGGCG	TTTCCAGCCG/gtgagtccct	2643 bp
5	119 bp	gtatttgcag/TGATTATTGA	AGACCCTTAC/gtaagataca	4232 bp
6	164 bp	ttttccatag/CTCTGGCTCG	3' UTR	

Fig. 6. Genomic structure, size of introns, and exon–intron splice junctions of the murine *nm23*-M5 gene. (A) Exon–intron distribution of *nm23*-M5. Exons are represented by black boxes. Intron sizes were estimated by PCR using primers located in cDNA sequences flanking the introns. The amplified DNA products were separated on an 0.8% agarose gel and stained with ethidium bromide. The molecular mass markers (1kb ladder, ATGene) are shown at the left of each panel. (B) All exon–intron splice junctions of the murine *nm23*-M5 gene follow the gt-at rule.

was highly increased by 4-folds in the CMV/*nm23*-M5-transfected cells (Fig. 7B). Considering that antioxidants protect cells against oxidative DNA damage, our results suggest that *nm23*-M5 plays an important role in both spermatogenesis and spermiogenesis by providing protection against damage induced by ROS.

Discussion

To clone genes with testis-specific expression that are involved in cellular redox regulation, we used a yeast-based genetic screening method [23]. This method allowed us to identify a number of testis-expressed genes that suppress the toxicity of *Bax* in yeast. The gene contained by the testis-12 clone conferred the highest tolerance to *Bax*-induced cell death. It was designated as the murine NDPK *nm23*-M5 on the basis of the alignment of its predicted amino acid sequence with those of other members of the family. A very high level of sequence similarity was found between this murine *nm23*-M5 cDNA and the human *Nm23*-H5 gene. The deduced amino acid sequences of these two proteins were also highly similar. In addition, both the Nm23-M5 and NM23-H5 proteins lack two important catalytic site residues and do not have NDPK activity (data not shown). Given the high level of similarity between these two proteins, it is possible that they not only share the same function, they may also have the same subcellular localization. This notion is supported by the phylogenetic analysis, which shows that Nm23-M5 and NM23-H5 group together.

We studied the expression of *nm23*-M5 in a variety of tissues and conclude that the expression of this gene is higher in male reproductive organs than in other tissues (Fig. 3B). Human *nm23*-H5 has the same expression pattern. However, unlike the human gene, we observed that *nm23*-M5 is expressed at higher levels in the adult testis than in the testes of young mice (Figs. 5A and B). Indeed, *nm23*-M5 expression was first detected at day 15 after birth, a time when primary spermatocytes in the early pachytene stage of meiosis are the most advanced germ cells present in the testis. Therefore, we are currently characterizing the expression patterns of the *nm23*-M5 and *nm23*-H5 genes more precisely to assess the differences in the expression of these two genes. We then found that high-level *nm23*-M5 expression is confined to late spermatids, depending on the stage of tubules, and is not observed outside of the testicular tubules. Hybridization with an antisense *nm23*-M5 RNA probe was focused on the neck region of late-stage spermatids. This could reflect the cell-specific and/or stage-specific expression of *nm23*-M5 to late-stage spermatids. In contrast, human *Nm23*-H5 expression is particularly localized in spermatogonia and early spermatocytes [8]. Thus, the murine *nm23*-M5 mRNA appears to be somewhat differently expressed than its human counterpart.

The BLAST program shows that the genomic *nm23*-M5 gene sequence partially aligns with sequences in a

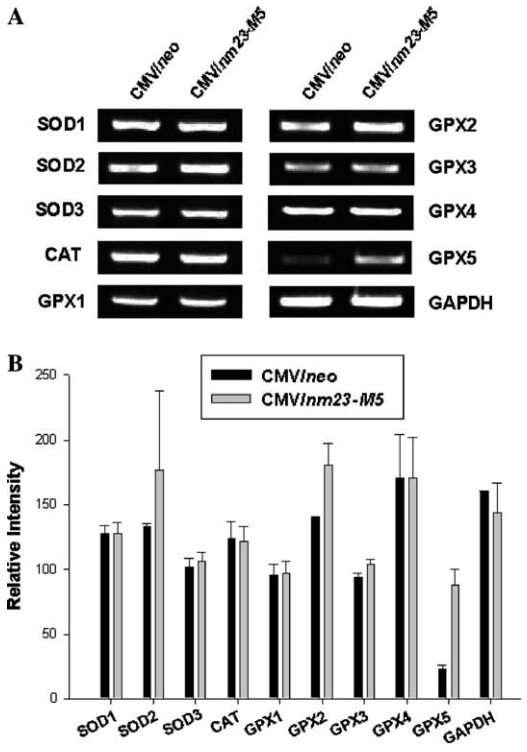

Fig. 7. RT-PCR analysis of the effect of *nm23*-M5 overexpression on transcript levels of antioxidant enzymes. (A) Expression level of antioxidant enzymes in control NIH3T3 cells (CMV/*neo*) and *nm23*-M5-overexpressing cells (CMV/*nm23*-M5). Cells were prepared by transient transfection (as described under "Materials and methods"). After 48 h of incubation, total RNA (2 μg) from CMV/*neo* and CMV/*nm23*-M5 cells was extracted and subjected to RT-PCR with specific primers for antioxidant enzymes (*SOD1*, *SOD2*, *SOD3*, *CAT*, *GPX1*, *GPX2*, *GPX3*, *GPX4*, and *GPX5*). RT-PCR for *GAPDH* was used as a loading control. (B) The level of gene expression is expressed as relative intensity. Data are shown as means + SD (bars) of triplicate determinations.

BAC library that was constructed from mouse chromosome 2 (Accession No. AC07335), indicating that *nm23*-M5 is located in chromosome 2. However, the human *nm23*-H5 gene mapped to chromosome 5q23–31 [8]. When we examined the mRNA expression of *nm23*-M5 by RT-PCR, three isoforms (Full, delE3, and delE3E4) could be amplified. Northern blot analysis, however, indicates that two (full and delE3) among three isoforms are detected (Figs. 3A and B). This difference between RT-PCR and Northern blot analysis suggested that delE3E4 expression is very low in testis, and that delE3 expression is only testis specific (Fig. 3B). Thus, our observations suggest that the *nm23*-M5 isoforms described in this study result from alternative splicing. The function of these *nm23*-M5 isoforms and how these isoforms are regulated is unclear.

NDPKs are multifunctional proteins that regulate a variety of eukaryotic cellular activities, including cell proliferation, development, and differentiation [1,3,5]. The mammalian NDPKs (EC 2.7.4.6) catalyze the transfer of γ-phosphates between nucleoside and deoxynucleoside di- and triphosphates. These proteins bear homology to each other in the NDPK domain. The Nm23-M5 protein differs from the other mammalian NDPK-like proteins in that its distribution is not ubiquitous. Furthermore, the recombinant GST-*nm23*-M5 fusion protein does not possess NDPK activity (data not shown). Thus, the function of *nm23*-M5 does not appear to be related to the normal roles played by the other NDPKs. A clue regarding the function of *nm23*-M5 is revealed by a very recent study that showed that the *AtNDPK2* gene plays a crucial role in the plant oxidative stress response [29]. *AtNDPK2* and *nm23*-M5 bear similarities to each other in their NDPK domains. This together with the identification of *nm23*-M5 as a gene that protects yeast from *Bax*-induced apoptosis suggests that *nm23*-M5 may protect developing male germ cells from being killed by cytotoxic oxidative stress. Supporting this notion is that when we transfected NIH3T3 cells with the CMV-*nm23*-M5 expression vector and analyzed the transcript levels of nine antioxidants, the expression of several antioxidant enzyme genes was found to be significantly increased. The expression of GPX5 was particularly profoundly upregulated. GPX5 is a 24-kDa secretory protein that acts independently of selenium and is expressed in the caput epididymidis under the control of androgens [30,31]. The protein has been shown to bind to the acrosomic region of spermatozoa in epididymus [32]. At that timing, GPX5 behaves in vivo and in vitro as a glutathione peroxidase [33]. Thus, we hypothesize that *nm23*-M5 controls the expression of GPX5 in some way and that this upregulation of antioxidant function serves to protect sperm membranes from oxidative damage.

In conclusion, we have cloned a new murine NDPK, *nm23*-M5, and characterized its function in the male reproductive tract. We believe that this gene functions to counter the effects of ROS, which can impair sperm function, by elevating the expression of antioxidant enzymes, including GPX5.

Acknowledgments

This work was partially supported by BioGreen21 from RDA and Agriculture special tax, Republic of Korea. K.C. Hwang and D.W. Ok are recipients of a scholarship from the BK21 program, granted by the Ministry of Education, Korea.

References

[1] D.L. Rosa, R.L. Williams, P.S. Steeg, *nm23*/nucleoside diphosphate kinase: toward a structural and biochemical understanding of its biological functions, Bio-Essays 17 (1995) 53–62.

[2] K. Nosaka, M. Kawahara, M. Masuda, Y. Satomi, H. Nishino, Association of nucleoside diphosphate kinase *nm23*-H2 with human telomeres, Biochem. Biophys. Res. Commun. 243 (1998) 342–348.

[3] K.J. Okabe, T. Kasukabe, Y. Honma, M. Hayashi, M. Hozumi, Purification of a factor inhibiting differentiation from conditioned medium of nondifferentiating mouse myeloid leukemia cells, J. Biol. Chem. 263 (1988) 10994–10999.
[4] E.H. Postel, S.J. Berberich, S.J. Flint, C.A. Ferrone, Human c-myc transcriptional factor PuF identified as *nm23*-H2 nucleoside diphosphate kinase, a candidate suppressor of tumor metastasis, Science 261 (1993) 478–480.
[5] D. Venturelli, R. Martinez, P. Melotti, I. Casella, C. Peschle, C. Cucco, G. Spampinato, Z. Darzynkiewicz, B. Calabretta, Over-expression of DR-*nm23*, a protein encoded by a member of the *nm23* gene family inhibits granulocyte differentiation and induces apoptosis in 32Dc13 myeloid cell, Proc. Natl. Acad. Sci. USA 92 (1995) 7435–7439.
[6] P.S. Steeg, G. Bevilacqua, L. Kopper, U.P. Thorgeirsson, J.E. Talmadge, L.A. Liotta, M.E. Sobel, Evidence for a novel gene associated with low tumor metastatic potential, J. Natl. Cancer Inst. 80 (1988) 200–204.
[7] L. Milon, M.F. Rousseau-Merck, A. Munier, M. Erent, I. Lascu, J. Capeau, M.L. Lacombe, *nm23*-H4, a new member of the family of human *nm23*/nucleoside diphosphate kinase genes, localised on chromosome16p13, Hum. Genet. 99 (1997) 550–557.
[8] A. Munier, C. Feral, L. Milon, V.P. Pinon, G. Gyapay, J. Capeau, G. Guellaen, M.L. Lacombe, A new human *nm23* homologue (*nm23*-H5) specifically expressed in testis germinal cells, FEBS Lett. 434 (1998) 289–294.
[9] A.M. Rosengard, H.C. Krutzsch, A. Shearn, J.R. Biggs, E. Barker, I.M. Margulies, C.R. King, L.A. Liotta, P.S. Steeg, Reduced Nm23/Awd protein in tumor metastasis and aberrant *Drosophila* development, Nature 342 (1989) 177–180.
[10] J.A. Stahl, A. Leone, A.M. Rosengard, L. Porter, C.R. King, P.S. Steeg, Identification of a second human *nm23* gene, *nm23*-H2, Cancer Res. 51 (1991) 445–449.
[11] M.L. Lacombe, L. Milon, A. Munier, J.G. Mehus, D.O. Lambeth, The human Nm23/nucleoside diphosphate kinases, J. Bioenerg. Biomembr. 32 (2000) 247–258.
[12] A.M. Gilles, E. Presecan, A. Vonica, L. Lascu, Nucleoside diphosphate kinase from human erythrocytes. Structural characterization of the two polypeptide chains responsible for heterogeneity of the hexameric enzyme, J. Biol. Chem. 266 (1991) 8784–8789.
[13] Y.H. Lue, A.P. Hikim, R.S. Swerdloff, P. Im, K.S. Taing, T. Bui, A. Leung, C. Wang, Single exposure to heat induces stage-specific germ cell apoptosis in rats: role of intratesticular testosterone on stage specificity, Endocrinology 140 (1999) 1709–1717.
[14] M.K. O'Bryan, S. Schlatt, D.J. Phillips, D.M. de Kretser, M.P. Hedger, Bacterial lipopolysaccharide-induced inflammation compromises testicular function at multiple levels in vivo, Endocrinology 141 (2000) 238–246.
[15] M. Hasegawa, G. Wilson, L.D. Russell, M.L. Meistrich, Radiation-induced cell death in the mouse testis: relationship to apoptosis, Radiat. Res. 147 (1997) 457–467.
[16] J.H. Richburg, The relevance of spontaneous- and chemically-induced alterations in testicular germ cell apoptosis to toxicology, Toxicol. Lett. 112–113 (2000) 79–86.
[17] H. Pfeifer, M. Conrad, D. Roethlein, A. Kyriakopoulos, M. Brielmeier, G.W. Bornkamm, D. Behne, Identification of a specific sperm nuclei selenoenzyme necessary for protamine thiol cross-linking during sperm maturation, FASEB J. 15 (2001) 1236–1248.
[18] P.C. Hsu, M.Y. Liu, C.C. Hsu, L.Y. Chen, Y.L. Guo, Effects of vitamin E and/or C on reactive oxygen species-related lead toxicity in the rat sperm, Toxicology 128 (1998) 169–179.
[19] C.G. Fraga, P.A. Motchnik, M.K. Shigenaga, H.J. Helbock, R.A. Jacob, B.N. Ames, Ascorbic acid protects against endogenous oxidative DNA damage in human sperm, Proc. Natl. Acad. Sci. USA 88 (1991) 11003–11006.
[20] N.J. Chinoy, R.R. Mehta, L. Seethalakshmi, J.D. Sharma, M.R. Chinoy, Effects of vitamin C deficiency on physiology of male reproductive organs of guinea pigs, Int. J. Fertil. 31 (1986) 232–239.
[21] K. Bensoussan, C.R. Morales, L. Hermo, Vitamin E deficiency causes incomplete spermatogenesis and affects the structural differentiation of epithelial cells of the epididymis in the rat, J. Androl. 19 (1998) 266–288.
[22] H. Moon, D. Baek, B. Lee, D.T. Prasad, S.Y. Lee, M.J. Cho, C.O. Lim, M.S. Choi, J. Bahk, M.O. Kim, J.C. Hong, D.J. Yun, Soybean ascorbate peroxidase suppresses *Bax*-induced apoptosis in yeast by inhibiting oxygen radical generation, Biochem. Biophys. Res. Commun. 290 (2002) 457–462.
[23] J. Sambrook, E.F. Fritsch, T. Maniatis, Molecular Cloning: A Laboratory Manual, Cold Spring Harbor Laboratory Press, Cold Spring Harbor, NY, 1989.
[24] L.M. Angerer, K.H. Cox, R.C. Angerer, Demonstration of tissue specific gene expression by in situ hybridization, Methods Enzymol. 152 (1987) 649–661.
[25] M.O. Kim, W.S. Choi, B.H. Lee, K.J. Cho, S.J. Seo, S.G. Kang, K.J. Kim, S.H. Baik, Localization and developmental changes of dopamine D1 and D2 receptor mRNAs in the rat brain, Korean J. Biol. Sci. 1 (1997) 497–505.
[26] J.H. Kim, H.S. Jung-Ha, H.T. Lee, K.S. Chung, Development of a positive method for male stem cell-mediated gene transfer in mouse and pig, Mol. Reprod. Dev. 46 (1997) 515–526.
[27] Aguilar-Mahecha, B.F. Hales, Robaire, B. Hales, Expression of stress response genes in germ cells during spermatogenesis, Biol. Reprod. 65 (2001) 119–127.
[28] T. Ikeya, A. Shinohara, S. Sato, S. Tabata, T. Ogawa, Localization of mouse *Rad51* and Lim15 proteins on meiotic chromosomes at late stages of prophase 1, Genes Cells 1 (1996) 379–389.
[29] H. Moon, B. Lee, G. Choi, D. Shin, D.T. Prasad, O. Lee, S.S. Kwak, D.H. Kim, J. Nam, J. Bahk, J.C. Hong, S.Y. Lee, M.J. Cho, C.O. Lim, D.J. Yun, NDP kinase 2 interaccts with two oxidative stress-activated MAPKs to regulate cellular redox state and enhances multiple stress tolerance in transgenic plants, Proc. Natl. Acad. Sci. USA 100 (2003) 358–363.
[30] N.B. Ghyselinck, C. Jimenez, J.P. Dufaure, Sequence homology of androgen-regulated epididymal proteins with glutathione peroxidase in mice, J. Reprod. Fertil. 93 (1991) 461–466.
[31] N.B. Ghyselinck, C. Jimenez, A.M. Lefrancois, J.P. Dufaure, Molecular cloning of a cDNA for androgen-regulated proteins secreted by the mouse epididymis, J. Mol. Endocrinol. 4 (1990) 5–12.
[32] P. Vernet, J. Faure, J.P. Dufaure, J.R. Drevet, Tissue and developmental distribution, dependence upon testicular factors and attachment to spermatozoa of GPX5, a murine epididymis-specific glutathione peroxidase, Mol. Reprod. Dev. 47 (1997) 87–98.
[33] P. Vernet, E. Rock, A. Mazur, Y. Rayssiguier, J.P. Dufaure, J.R. Drevet, Selenium-independent epididymis-restricted glutathione peroxidase 5 protein (GPX5) can back up failing SE-dependent GPXs in mice subjected to selenium deficiency, Mol. Reprod. Dev. 54 (1999) 362–370.
[34] A.R. Bellve, C.F. Millette, Y.M. Bhatnagar, D.A. O'Brien, Dissociation of the mouse testis and characterization of isolated spermatogenic cells, J. Histochem. Cytochem. 25 (1977) 480–494.